

# DEVELOPMENT OF INNER-SPHERICAL CONTINUOUSLY VARIABLE TRANSMISSION FOR BICYCLES

M. W. PARK<sup>1)</sup>, H. W. LEE<sup>2)\*</sup>, N. G. PARK<sup>2)</sup> and H. S. SANG<sup>3)</sup>

<sup>1)</sup>Department of Mechanical Design Engineering, Graduate School, Pusan National University, Busan 609-735, Korea

<sup>2)</sup>School of Mechanical Engineering, Pusan National University, Busan 609-735, Korea

<sup>3)</sup>School of Fire & Disaster Prevention, Kyungil University, Gyeongbuk 712-701, Korea

(Received 21 November 2006; Revised 26 August 2007)

**ABSTRACT**—A new continuously variable transmission for bicycles (B-CVT) is developed by using a traction drive mechanism having inner and outer spherical rotors. The B-CVT has high power efficiency, large torque capacity, improved drivability and good packageability. The ratio change mechanism for the B-CVT is very simple, in contrast with other traction drive CVTs. After completing a conceptual design, a performance analysis and a detail design, a prototype of the B-CVT has been manufactured. The prototype has rated power of 100 watts, pedal speed of 6 rad/s and an overall speed ratio of 1.0–4.0. A bench test and an actual bicycle test have been performed to verify the practicability of the B-CVT.

**KEY WORDS** : Continuously variable transmission (CVT), Inner spherical continuously variable transmission (ISCVT), Traction drive, Bicycle

## NOMENCLATURE

$\eta$	: power efficiency of the ISCVT traction drive
$\omega_1, \omega_2$	: speed of the driving and driven rotors
$T_1, T_2$	: torque of the driving and driven rotors
$r_1, r_2, r_c$	: radii of the driving, driven and counter rotors
$h$	: installed height of a bearing pedestal on the frame
$\phi$	: tilting angle of a rotating axis of the counter rotor
$\theta$	: contact angle between the driving/driven and counter rotors
$r_{p1}$	: cam pitch radius of the pressure device
$\lambda$	: cam inclination angle of the pressure device
$\delta$	: speed ratio of the ISCVT
$N_1$	: normal force on the contact area between the driving and counter rotors

## 1. INTRODUCTION

Most commercial bicycles use a chain-shift transmission, although variants employing gears and/or belt-pulleys also exist. The unique constraints on bicycle design have a large influence on the choice of transmission. Since the motive power is supplied by a human, it is desirable for the efficiency to exceed 90%; otherwise, the rider may

sense the relatively low efficiency and become dissatisfied. Since a bicycle transmission is installed in a narrow and limited space such as the side of a pedal, the rear wheel or the inside of a hub, a compact transmission with a high power capacity is required for bicycles. Because of these constraints, the chain-shift transmission has been recognized as the most proper model for bicycle transmissions. This design has several disadvantages, however. The delay in changing speed ratio is relatively long, and the chain sometimes derails from the sprockets. Both of these problems cause drivability to be poor. In addition, the average utilization of each chain-shift is less than 40% because the speed ratios are biased or even redundant (Chang *et al.*, 1999).

Much research and development work has been applied to chain-sprockets, gears and/or continuously variable transmissions (CVT) to overcome these disadvantages, but remarkable outcomes have not been demonstrated to date. In the case of a chain-sprocket, an automatic derailleur has been developed for the rider's convenience, but it is expensive and complicated. In the case of a gear system, it is desirable to develop a ratio changer with a simple, economical design. In the case of a CVT, designers should emphasize power efficiency and packageability. On the other hand, for well-known designs such as the push-belt or toroidal drive it is very difficult to obtain a feasible model that satisfies the constraints.

\*Corresponding author. e-mail: leehwoo@pusan.ac.kr

In this work, we apply a new CVT to bicycle transmissions with a traction drive that transmits power through contacts between an inner sphere and an outer sphere (inner-spherical CVT; ISCVT). The ISCVT has been shown to be practical when applied to scooter and automotive transmissions (Ryu *et al.*, 2004; Ku *et al.*, 2004). The application of a ISCVT to a bicycle is more suitable than any other types of CVT in the areas of efficiency, power capacity and packageability (Park *et al.*, 2005; Seong *et al.*, 2005). The B-CVT has no shifting chain-sprockets; instead, a manually controlled mechanical ratio changer has been developed. The B-CVT has a rated power and speed of 100 watts and 6 rad/s respectively and an overall speed ratio of 1.0~4.0. A bench test has been carried out to evaluate power efficiency, and an actual bicycle test has been performed on level and uphill roads to verify the practicability of the B-CVT.

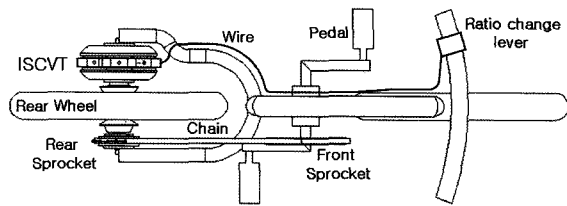


Figure 1. Mechanism layout of the B-CVT.

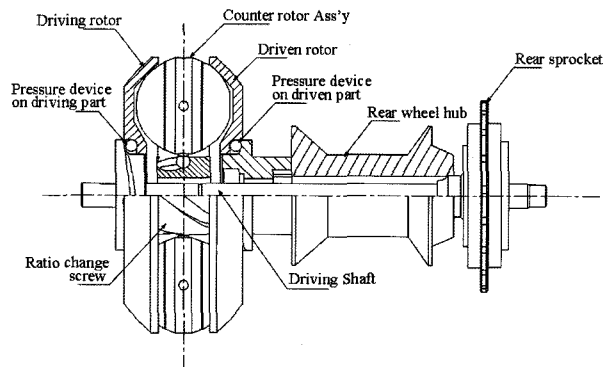


Figure 2. A Section view of the ISCVT assembled into the rear wheel hub.

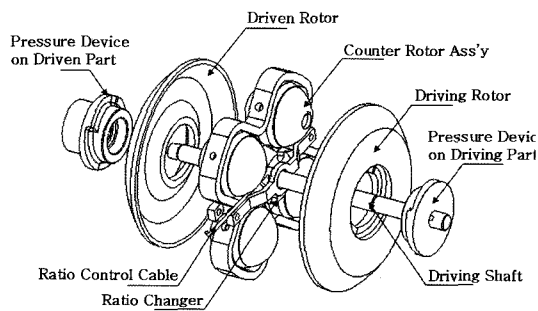


Figure 3. Components of the ISCVT.

## 2. ISCVT FOR BICYCLES

### 2.1. Mechanism Layout

Figure 1 shows the mechanism layout of the B-CVT using the ISCVT. The B-CVT consists of chain-sprockets, an ISCVT assembly and a speed ratio change mechanism. The chain-sprockets connecting the pedal to the driving shaft of the ISCVT are arranged with a fixed gear ratio, and a one-way clutch is installed in the inner face of the rear sprocket. Instead of chain-sprockets, belt-pulleys can be replaced without any driveability change. The ISCVT is installed on the side of the rear wheel, where it attaches the wheel to an output shaft. The speed ratio change mechanism is equipped with the screw-balls ratio changer inside the ISCVT and a lever connected to the screw-balls ratio changer by a wire. Figure 2 shows a section view of the ISCVT assembly as assembled into the rear wheel hub.

### 2.2. Features of the ISCVT

Figure 3 represents components of the ISCVT assembly consisting of a traction drive variator, two pressure devices and the screw-balls ratio changer. The traction drive variator consists of a driving, a driven and 4 counter rotors having an inner and outer spherical surface. Power is transmitted through the driving shaft across the hub from the rear sprocket into the input rotor of the ISCVT assembly.

#### 2.2.1. Traction drive

Power transmission is performed by the high shear resistance of the lubricant, which exists as a thin oil film between two rolling contact areas of the rotors. The lubrication, known as EHL (elasto-hydrodynamic lubrication), transmits power through the thin oil film and improves CVT lifetime (Heilich and Shube, 1983). Because the inner and outer spherical contact of the

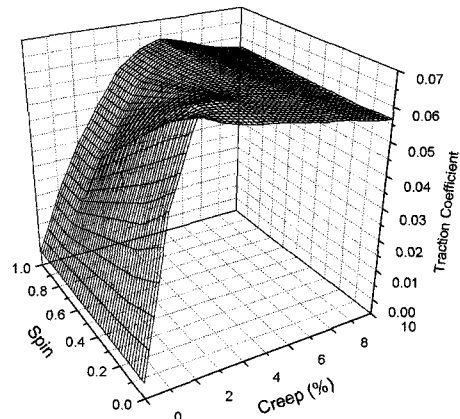


Figure 4. Traction coefficients of the traction lubricant (SANTOTRAC-50).

ISCVT reduces stress on the rolling contact area, fatigue resistance is increased and torque capacity is maximized in comparison with the Toroidal, Kopp-Ball, Milner or Disk type CVT. In addition, because the inner and outer spherical contact is circular and reduces spin loss, the power efficiency is improved (Ryu *et al.*, 2004).

The power efficiency of the ISCVT traction drive is calculated as

$$\eta = \frac{\omega_2 T_2}{\omega_1 T_1} \quad (1)$$

where the values of  $\omega_2$  (speed of the driven rotor) and  $T_2$  (speed torque of the driven rotor) are determined from the equilibrium equations for axial torque on the two rolling contact areas of the rotors;  $\omega_2$  and  $T_2$  are calculated from Equations (2), (3) and (4) (Seong *et al.*, 2005). The contact areas are lubricated by the synthesis lubricant SANTOTRAC-50, which has traction coefficients as shown in Figure 4.

$$\int_{A_1} (\mathbf{r}_1 + \boldsymbol{\rho}_1) \times \boldsymbol{\tau}_1 dA_1 - T_1 = 0 \quad (2)$$

$$\int_{A_1} (\mathbf{r}_1 + \boldsymbol{\rho}_1 + \mathbf{a}_1) \times \boldsymbol{\tau}_1 dA_1 + \int_{A_2} (\mathbf{r}_2 + \boldsymbol{\rho}_2 + \mathbf{a}_2) \times \boldsymbol{\tau}_2 dA_2 = 0 \quad (3)$$

$$\int_{A_2} \int_{A_1} (\mathbf{r}_2 + \boldsymbol{\rho}_2) \times \boldsymbol{\tau}_2 dA_2 - T_2 = 0 \quad (4)$$

The contact stress of the rolling contact areas is calculated by Hertz contact theory (Pillkey, 1994), and fatigue life is determined from Lundberg-Palmgren theory (Rohn *et al.*, 1981).

### 2.2.2. Pressure device

The frontal pressure device generates a normal force in the contact area between the driving rotor and the frontal counter rotor. The rear pressure device generates sufficient normal force to avoid slip between the rear counter rotor and the driven rotor. Each contact force is

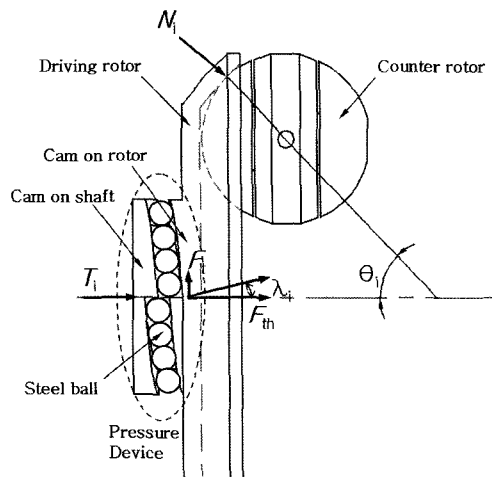


Figure 5. Schematics of the pressure device.

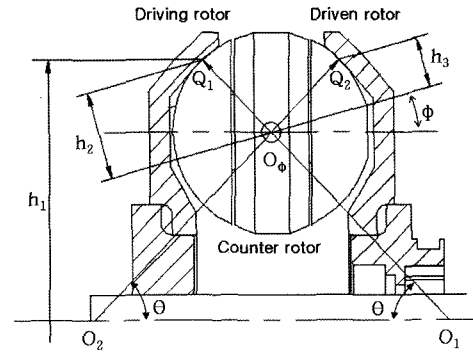


Figure 6. Kinematic diagram of the ISCVT.

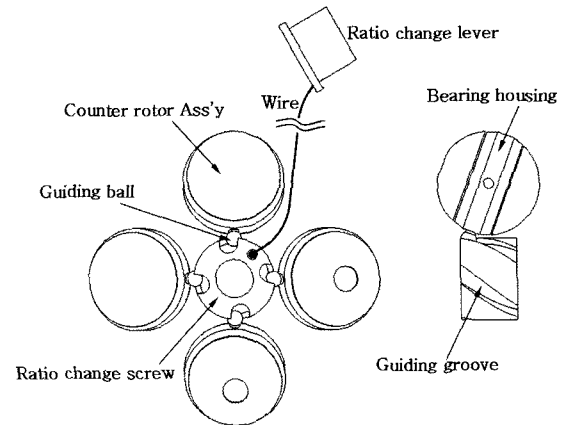


Figure 7. Schematics of the ratio change mechanism.

proportional to an associated shaft torque. Figure 5 shows the pressure device on the driving rotor. The pressure device is equipped with cams on the rotor and shaft and several steel balls between the cams. A thrust force is generated from an input torque by the loading cams of the pressure device, and the thrust force induces a normal force on the contact point of the driving rotor. The relationship between the input torque and normal force is given as follows:

$$N_1 = \frac{T_1 / r_{p1}}{\tan \lambda \cos \theta_1} \quad (5)$$

### 2.2.3. Ratio change mechanism

The ISCVT changes speed continuously by altering the tilting angle of a rotating axis of each counter rotor between the driving and driven rotors. The speed ratio of the ISCVT is defined as the driven rotor speed versus the driving rotor speed. Referring to Figure 6, the speed ratio is expressed as an equation with radii ( $h_2$ ,  $h_3$ ) of contact points ( $Q_1$ ,  $Q_2$ ) to the rotating axis tilted as an angle of  $\phi$  and given as follows:

$$\delta = h_3 / h_2 \quad (6)$$

where

Table 1. Design specifications.

Rated power	100 watt
Rated input pedaling speed	6.0 rad/s
Overall speed ratio	1.0~4.0
Sprocket gear ratio	2.0

Table 2. Design procedure.

1. Input the rated power and input speed
2. Choose values based on geometrical parameters defining the mechanism layout
3. Calculate bounds of the variable tilting angle of the counter rotor rotating axis based on bounds of the overall speed ratio
4. Check whether there is sufficient space to install the ratio change screw in the center part of the ISCVT
5. Estimate an overall diameter and width of the ISCVT and check whether the size is within prescribed values
6. Choose a cam inclination angle as the main parameter of the pressure device
7. Calculate contact stresses and lifetimes and check whether stresses are within the allowable limit
8. Calculate power efficiency based on tribology analysis
9. Select the best solution among obtained feasible solutions

Table 3. Design constraints.

	$r_1, r_2$	$r_1 = r_2 \leq 120$ mm
Variable constraints	$r_c$	$r_c \leq 35$ mm
	$h$	$30 \leq h \leq 45$ mm
	$\lambda$	$\lambda \leq 15^\circ$
Installation constraints	Overall size	$\Phi 200 \times 70$ mm
	Ratio change screw diameter	$\Phi(h-5)$ mm
Performance constraints	Efficiency	85%
	Shear stress	500 Mpa
	Fatigue life	1 Ghour

Table 4. Design results.

Variables		Performance	
$r_1, r_2$	72 mm	Efficiency	92%
$r_c$	20.2 mm	Max. shear stress	450 Mpa
$h$	37.4 mm	Fatigue life	74.3 Ghour
$\tilde{\epsilon}$	$6^\circ$	Overall size	$\Phi 145 \times 66$ mm

$$h_2 = r_c \sin(\theta + \phi) \tag{7}$$

$$h_3 = r_c \sin(\theta - \phi) \tag{8}$$

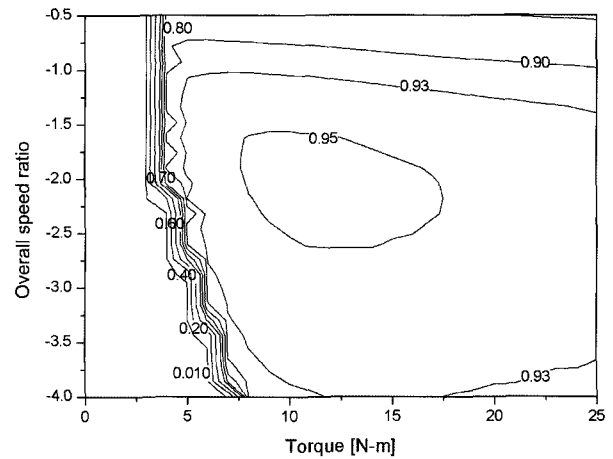


Figure 8. Efficiency distribution at the rated speed.

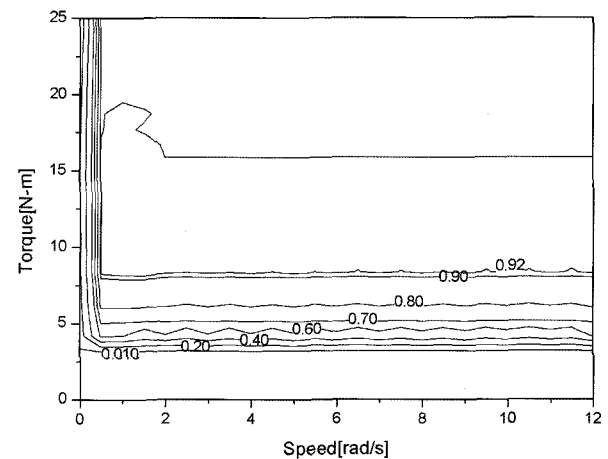


Figure 9. Average efficiency over the range of practical pedal speeds.

Figure 7 shows the ratio change mechanism, which consists of the ratio change screw, wire, back-spring and lever. The screw is made by grooving four helical lines. A guiding ball is inserted into the guiding groove. As the screw is rotated with respect to the driving/driven rotor rotating axis, the bearing housings of the counter rotor assemblies are tilted with respect to the perpendicular direction on the rotor driving/driven rotor rotating axis. To rotate the screw, the wire is pulled or released by the lever operation.

### 3. CONCEPTUAL DESIGN

To verify practicability of the proposed ISCVT for bicycles, design specifications listed in Table 1 were chosen and a conceptual design was developed. Table 2 shows the design procedure used to obtain feasible solutions satisfying the given design constraints sum-

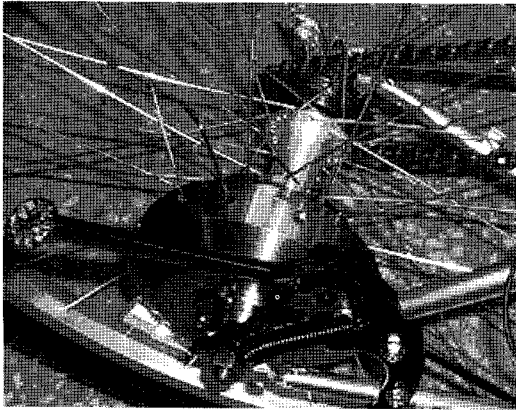


Figure 10. B-CVT installed in a commercial bicycle.

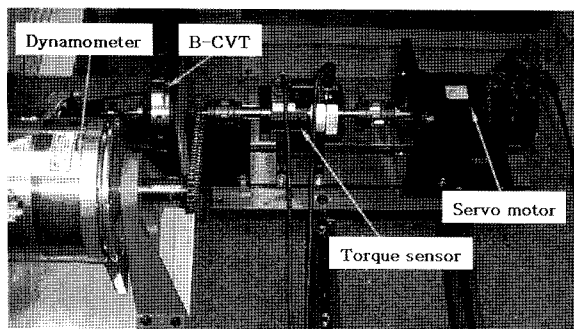


Figure 11. Test-bench for B-CVT.

marized in Table 3.

The design variables considered in the optimization process include the radii ( $r_1$ ,  $r_2$ ,  $r_c$ ) of inner and outer sphere on the driving/driven and counter rotors respectively, installed height ( $h$ ) of a bearing pedestal on the frame, and cam inclination angles ( $\lambda$ ) of the pressure devices. The most efficient feasible solution, whose parameters are specified in Table 4, was selected as the best solution. The overall diameter and width of 145 and 66 mm, respectively, are small enough to allow installation inside the rear wheel.

Shown in Figure 8 is the power efficiency distribution at a pedaling speed of 6.0 rad/sec for the most efficient design. In most of the region over 6.0 N-m, efficiencies are over 90%. Figure 9 shows average values in the range of practical pedal speed. The variation is very slight and the values are consistently near 90% efficiency. At the rated power level, the maximum shear stress acting on the contact area between the spherical rotors is 450 MPa. The theoretically estimated fatigue life is calculated as 74.3 G-hour based on the Lundberg-Palmgreen theory.

## 4. PROTOTYPE EVALUATION

### 4.1. Prototype Manufacturing

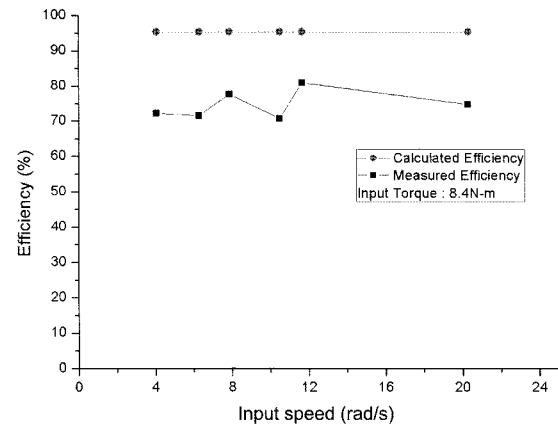


Figure 12. A comparison of measured and calculated efficiency.



Figure 13. Road test for B-CVT.

Based on the results of the optimal design listed in Table 3, we developed a detailed design to determine bearing selection and machined element dimensions. A solid model for a prototype was constructed with commercial CAD software. Chromium-molybdenum alloy steel (AISI4140) was selected as the prototype material. (Harvey, 1985) The prototype was installed in a commercial bicycle as shown in Figure 10.

### 4.2. Power Efficiency Test

Figure 11 shows a test rig to measure the power transmission efficiency of the B-CVT. The test rig consisted of a power source (AC servo motor), torque sensor, photo sensor and dynamometer. The driving shaft of the B-CVT was directly connected to the torque sensor and the driven shaft was connected to the dynamometer by a chain-sprocket mechanism with a fixed ratio of 1:1. The test was carried out in driving conditions at an overall speed ratio of 2.0, an 8.4 N-m rated input torque and variable input speed. The measured efficiencies of the test are shown in Figure 12. Power efficiency is seen to be greater than 80% at the rated input speed. The

difference between measured and calculated efficiency is approximately 10~20%. This difference can be attributed to manufacturing error of the rotors, bearing loss and unstable lubricant conditions. The trends between the measured and calculated results are nevertheless similar.

#### 4.3. Road Test

An actual bicycle test was performed on level and uphill roads to verify the practicability of the B-CVT. Figure 13 shows a scene from the road test in which a commercial bicycle was ridden while equipped with the B-CVT. The maximum acceleration was calculated to be approximately  $0.7 \text{ m/s}^2$  at a level road condition. The gradability in climbing the uphill road was measured as 5.2%. According to the Guide for the Development of Bicycle Facilities (Flowers *et al.*, 1999), these acceleration and gradability results are considered good enough to apply for commercial development of the proposed model.

### 5. CONCLUSIONS

To improve drivability of a bicycle, the new ISCVT is designed for general-purpose bicycles. Based on a design process that considered the various constraints on efficiency, stress, fatigue life and dimensions, an optimal design was chosen and a prototype was constructed. Based on the test results, the following conclusions are drawn:

- (1) Feasible solutions with the relatively small dimensions of  $\Phi 145 \times 66 \text{ mm}$  can be obtained.
- (2) Power efficiency is measured to be greater than 80% at the rated input speed and torque.
- (3) The maximum acceleration is calculated to be approximately  $0.7 \text{ m/s}^2$ .
- (4) The gradability in climbing an uphill road is measured to be 5.2%.
- (5) The possibility of producing the transmission as a commercial good has been demonstrated.

### REFERENCES

- Cho, C. K., Yun, M. H., Yoon, C. S. and Lee, M. W. (1999). An ergonomic study on the optimal gear ratio for a multi-speed bicycle. *Int. J. Industrial Ergonomics*, **23**, 95–100.
- Flowers, D., Warne, T. R. and Pyers, C. E. (1999) Guide for the development of bicycle facilities. *American Association of State Highway and Transportation Officials*. Washington.
- Harvey, P. D. Editor (1985). *Engineering Properties of Steel*. American Society for Metals. 2nd edn.. Metals Park. Ohio.
- Heilich, F. W. and Shube, E. E. (1983). *Traction Drives: Selection and Application*. Mechanical Engineering Series. Marcel Dekker. New York.
- Ku, I. K. and Park, N. G. (2004). An introduction of a new traction drive pairing with the inner and the outer surface of the spherical rotors for automobile usage. *Int. Continuously Variable and Hybrid Transmission Congress*, 431–438.
- Park, M. U. and Park, N. G. (2005). Development of new continuously variable transmission for bicycles. *SAE Paper No. 2005-03-0113*.
- Pillkey, W. D. (1994). *Formulas for Stress, Strain and Structural Matrices*. John Wiley & Sons. New York.
- Rohn, D. A., Loewenthal, S. H. and Coy, J. J. (1981). Simplified fatigue life analysis for traction drive contacts. *ASME J. Mechanical Design* **103**, **1**, 430–439.
- Ryu, J. H., Kim, J. H. and Park, N. G. (2004). Development of the inner spherical traction CVT for scooters. *Fall Conf. Proc., Korean Society of Automotive Engineers*, 577–581.
- Seong, S. H., Ryu, J. H. and Park, N. G. (2005). Conceptual design of inner-spherical continuously variable transmission for bicycle usage. *Int. J. Automotive Technology* **6**, **5**, 467–473.